J Incl Phenom Macrocycl Chem (2009) 63:203–210
DOI 10.1007/s10847-008-9508-3

ORIGINAL ARTICLE

Inclusion of amides by a fluorenyl diol host

Elise J. C. de Vries · Luigi R. Nassimbeni · Edwin Weber

Received: 31 July 2008 / Accepted: 29 September 2008 / Published online: 25 November 2008

Abstract The structure of the host compound 1,4-bis (9-hydroxy-9-fluorenyl)benzene as well as the structures of the inclusion complexes with four amides, dimethylformamide (DMF), dimethylacetamide (DMA), tetramethylurea (TMU) and hexamethylphosphoramide (HMPA) have been elucidated. Each structure crystallised in a centrosymmetric space group with $Z = 2$ and a host to guest ratio of 1:1 or 1:2, as determined by thermogravimetric analysis. Lattice energies have been calculated by atom-atom potential methods and these results were compared to the thermal stabilities observed.

Keywords Inclusion complex · Thermal analysis · Lattice energies

Introduction

The compound 1,4-bis(9-hydroxy-9-fluorenyl)benzene, H, is a typical wheel and axel or dumbbell shaped host containing bulky, substituents separated by a spacer. The hydroxyl moieties make them especially efficient hosts, as these act as hydrogen bond donors to guests which have suitable H-bond acceptors. The best known example is the host 1,1,6,6-tetraphenylhexa-2,4-diyne-1,6-diol, which has been studied extensively [1–3]. The fluorenyl host, H, is one of a series that have been synthesised [4], and conforms to Weber's rules of host design of rigidity and topology in order to yield coordinato-clathrates [5, 6]. Bacchi et al. [7, 8] have extended this design concept by incorporating metals into the spacer and has proposed a "venetian blinds" mechanism to explain the process of solvation/desolvation that such compounds display with volatile guests.

This paper reports on the investigation of the enclathration of four amide guests by the host. The amides investigated were dimethylformamide (DMF), dimethylacetamide (DMA), tetramethylurea (TMU) and hexamethylphosphoramide (HMPA). We describe the structure of the host as well as the structures of the inclusion compounds formed by the host and the four amides mentioned. Furthermore an investigation of the trend in thermal stability and lattice energies of the complexes was explored. The atomic numbering scheme of both host and the respective guests is shown in Fig. 1.

E. J. C. de Vries (✉) · L. R. Nassimbeni
Department of Chemistry, University of Cape Town, Rondebosch 7701, Cape Town, South Africa
e-mail: dvreli002@uct.ac.za

L. R. Nassimbeni
e-mail: luigi.nassimbeni@uct.ac.za

E. Weber
Institut für Organische Chemie, Technische Universität Bergakademie Freiberg, Leipziger Strasse 29, 09596 Freiberg, Sachsen, Germany

Experimental section

Crystallisation

Crystals of the host were obtained by dissolving it in a minimum amount of heated chloroform and leaving the vial to undergo slow evaopration. Similarly, crystals of the inclusion complexes were obtained by dissolving the host in a minimum amount of a heated solution of the respective

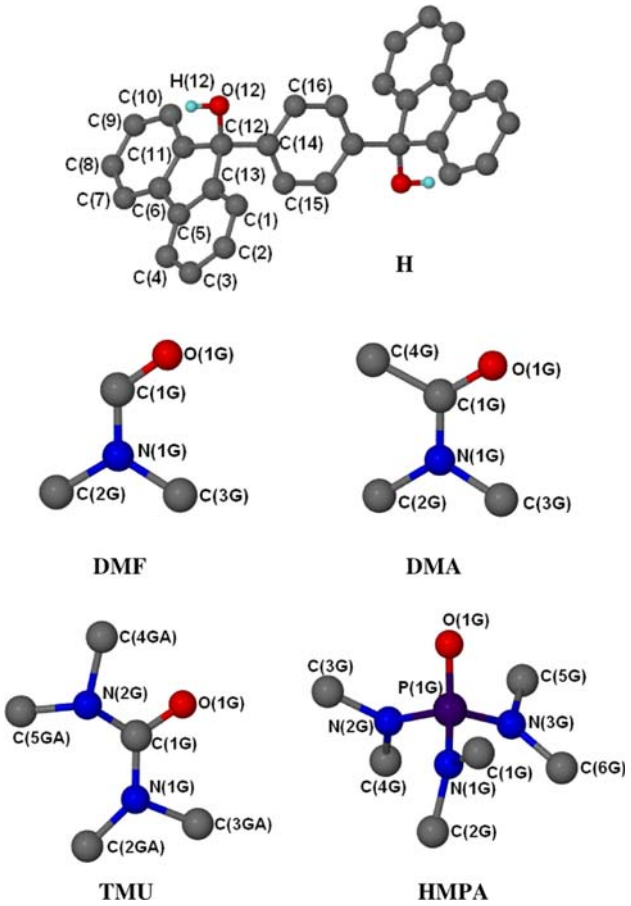

Fig. 1 Numbering of the host and guest molecules. All hydrogen atoms, except the hydroxyl hydrogen atom, are omitted for clarity

guest. The resulting unfiltered solutions were left at room temperature to undergo slow evaporation.

Data collection

Cell dimensions were established from the intensity data measured on a Nonius Kappa CCD diffractometer using graphite-monochromated MoKα radiation from crystals coated with Paratone N oil. All data was collected at low temperature (183 K). Data collection (COLLECT software) [9] involved a combination of ϕ- and ω-scan techniques. The program DENZO-SMN [10] was used for unit cell refinement and data reduction. Crystallographic data are presented in Table 1.

Structure solution and refinement

The structures were solved by direct methods using SHELX-86 [11] and refined by least squares with SHELX-97 [12] refining on F^2. The program X-Seed [13, 14] was used as a graphical interface for structure solution and refinement. Direct methods yielded the positions of the non-hydrogen atoms. These non-hydrogen atoms were refined anisotropically. The hydroxyl hydrogen atoms were located in the difference electron density map and refined with simple bond length constraints. All remaining hydrogens were placed with geometric constraints. All hydrogen atoms were assigned isotropic temperature factors of $1.2U_{eq}$ of their parent atom. In the H·2TMU structure the $-CH_3$ are disordered over two positions and modelled accordingly. To maintain appropriate bond distances constraints were placed on the N–C bonds. This value was obtained by averaging the N–CH_3 bond lengths found in the other three structures.

Thermal analysis

Both differential scanning calorimetry (DSC) and thermogravimetric analysis (TGA) were performed on a Perkin Elmer PC7-Series instrument. The samples were crushed and blotted dry (2–4 mg) and placed in crimped, vented aluminium DSC pans or open aluminium TGA sample pans. The experiments were performed over a temperature range of 30–300/350 °C at a heating rate of 10 or 20 °C min^{-1} under dry nitrogen with a flow rate of 30 mL min^{-1}.

Lattice energy calculations

Lattice energy calculations were performed using the *ZIPOPEC* module of the *OPIX* program suite [15]. The functional form for the i–j atom-atom potential used is

$$E_{ij} = A \cdot \exp(-BR_{ij}) - C/R_{ij}^6$$

where R_{ij} is the interatomic distance and the coefficients A, B and C have been carefully normalised against the known sublimation energies of selected organic compounds. The atomic coordinates of a carefully chosen selected reference molecular group were input into the program and the appropriate summations of all host–host, host–guest and guest–guest interactions were calculated for each structure.

Results and discussion

Structures

Crystallographic data and experimental refinement parameters are given in Table 1. The apohost, obtained from a solution of chloroform, crystallised in the space group P $\overline{1}$ with $Z = 2$. Two half host molecules (denoted

Table 1 Crystal data and structure refinement parameters

	H	H·DMF	H·DMA	H·2TMU	H·2HMPA
Empirical formula	$C_{32}H_{22}O_2$	$C_{32}H_{22}O_2{\cdot}C_3H_7ON$	$C_{32}H_{22}O_2{\cdot}C_4H_9ON$	$C_{32}H_{22}O_2{\cdot}2(C_5H_{12}ON_2)$	$C_{32}H_{22}O_2{\cdot}2(C_6H_{18}ON_3P)$
Molar ratio		1:1	1:1	1:2	1:2
Formula weight (g mol^{-1})	438.5	511.59	525.62	670.83	796.9
Crystal system	Triclinic	Triclinic	Triclinic	Monoclinic	Monoclinic
Space group	P-1	P-1	P-1	$P2_1/c$	$P2_1/n$
a(Å)	8.4559(4)	9.0106(9)	8.9141(4)	8.4595(2)	11.8642(6)
b(Å)	10.8676(6)	12.0117(15)	12.5243(7)	12.7944(5)	14.2552(10)
c(Å)	13.4376(10)	13.6841(16)	13.7726(9)	17.0672(8)	13.3132(8)
α(°)	94.616(4)	106.656(4)	108.112(3)	90	90
β(°)	91.769(4)	101.429(5)	99.687(3)	99.805(3)	108.847(3)
γ(°)	111.509(3)	101.321(6)	103.014(3)	90	90
Volume (Å^3)/Z	1142.70(12)/2	1339.3(3)/2	1375.95(13)/2	1820.27(12)/2	2130.9(2)/2
$D_{(calc)}$ (g cm^{-3})	1.274	1.269	1.269	1.224	1.242
μ(MoKα) (mm^{-1})	0.078	0.080	0.080	0.079	0.151
F(000)	460	540	556	716	852
Temperature (K)	183(2)	183(2)	183(2)	183(2)	183(2)
Dimensions (mm)	0.23 × 0.12 × 0.12	0.25 × 0.20 × 0.05	0.32 × 0.12 × 0.10	0.30 × 0.21 × 0.15	0.15 × 0.10 × 0.08
θ-range collection	3–26	2–26	2–27	3–27	2–25
Index range	$-10 \le h \le 10$	$-10 \le h \le 10$	$0 \le h \le 11$	$0 \le h \le 10$	$-14 \le h \le 14$
	$-13 \le k \le 13$	$-14 \le k \le 14$	$-15 \le k \le 15$	$0 \le k \le 16$	$-16 \le k \le 16$
	$-16 \le l \le 16$	$-16 \le l \le 16$	$-17 \le l \le 16$	$-21 \le l \le 21$	$-15 \le l \le 15$
Reflections collected	4346	5020	5897	3950	3749
Independent reflections	2859	2452	3507	2680	2253
Number of parameters	313	360	370	235	256
R_{int}	0.0747	0.0733	0.0000	0.0000	0.0588
Goodness of fit, S	1.012	0.972	1.024	1.067	1.005
R_1 [$I > 2\sigma(I)$]	0.0402	0.0497	0.0523	0.0779	0.0496
wR_2	0.0855	0.0995	0.1161	0.2020	0.1121
Largest diffraction peak and hole (e Å^{-3})	0.16 and −0.22	0.21 and −0.24	0.70 and −0.29	0.62 and −0.58	0.20 and −0.28

Table 2 Hydrogen bonding data for the host and the inclusion complexes

	Donor–H···Acceptor	D–H (Å)	H···A (Å)	D···A (Å)	D–H···A (°)
H	O(12A)–H(12A)···O(12B)	0.90(2)	1.92(2)	2.79(1)	163(1)
H·DMF	O(12A)–H(12A)···O(1G)	0.82(2)	1.99(3)	2.81(1)	180(3)
	O(12B)–H(12B)···O(1G)	0.88(3)	1.91(3)	2.79(1)	171(2)
H·DMA	O(12A)–H(12A)···O(1G)	0.85(2)	1.89(2)	2.74(1)	176(2)
	O(12B)–H(12B)···O(1G)	0.86(2)	2.07(2)	2.92(1)	170(2)
H·2TMU	O(12)–H(12)···O(1G)	0.92(3)	1.81(3)	2.72(1)	178(3)
H·2HMPA	O(12)–H(12)···O(1G)	0.84(3)	1.94(3)	2.78(1)	175(3)

A and B) comprises the asymmetric unit and are located on centres of inversion at Wyckoff positions *a* and *g*. Molecule A is hydrogen bonded to molecule B by an O–H···O hydrogen bond (Table 2). The hydroxyl hydrogen atom on molecule B is not involved in hydrogen bonding. The hydrogen bonding generates chains of

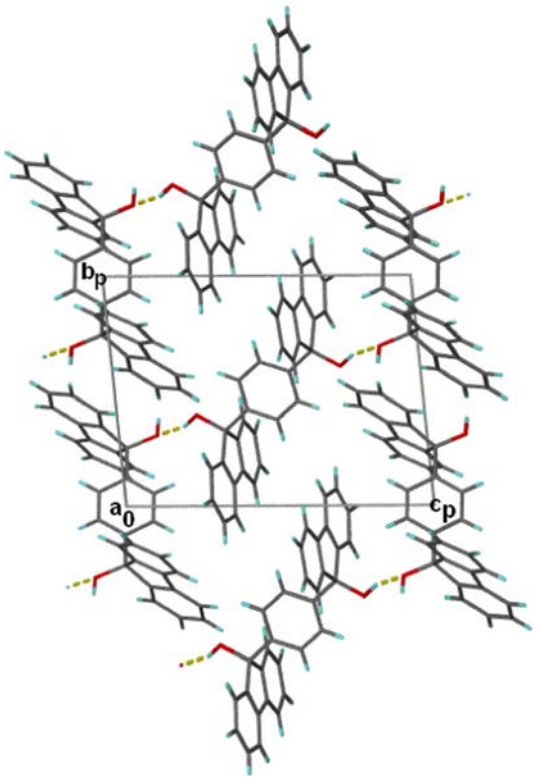

Fig. 2 Packing diagram of H down [100] shows the hydrogen bonding

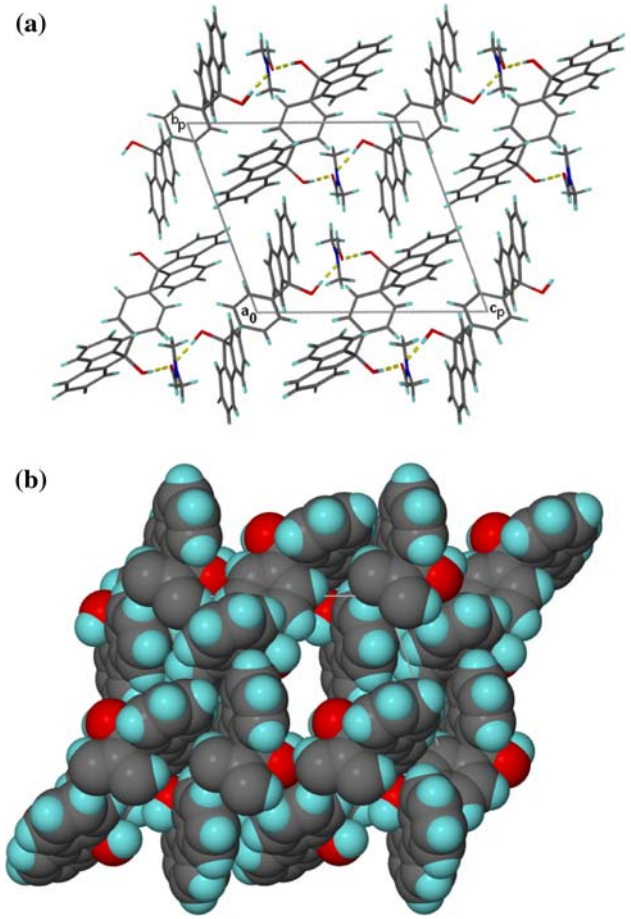

Fig. 3 **a** Packing diagram of H·DMF down [100] shows the chains generated by the double acceptor hydrogen bonding capability of the guest (**b**) space-filling projection down [100] with guest molecules omitted, showing the channels

alternating host molecule A and B that run parallel to [01-1], Fig. 2.

The complexes H·DMF and H·DMA are isostructural with respect to the host molecule and crystallise with a molar ratio of 1:1 in the space group P $\overline{1}$ with $Z = 2$. Two half host molecules (denoted A and B) and one guest molecule comprises the asymmetric unit. The two half host molecules are located on centres of inversion at Wyckoff positions *a* and *b*, with the guest in a general position. The structure is stabilised by two independent (host) O–H···O (guest) hydrogen bonds (Table 2). Both DMF and DMA therefore act as a double hydrogen bond acceptor molecule. This gives rise to endless chains of alternating, hydrogen bonded, host and guest molecules (Fig. 3a). The orientation of the chains is parallel to the *c*-axis. The chains stack upon each other generating channels running down [100] in which the guests are located (Fig. 3b).

The complexes H·2TMU and H·2HMPA crystallise in the space group $P2_1/c$ and $P2_1/n$ respectively with $Z = 2$. In both structures the asymmetric unit consists of half a host molecule and one guest molecule. The host lies on a centre of inversion at Wyckoff position *a* in the H·2TMU complex and in position *c* in the H·2HMPA complex. In both structures the guest is located in a general position. Both guests act as single acceptor guests which results in a distinct supramolecular host–guest entity with 1:2 stoichiometry. The host molecules pack to form channels in which the guests are located. These channels run parallel to [100] and [001] in H·2TMU (Fig. 4) and H·2HMPA (Fig. 5), respectively. The difference in the packing modes is due to the C(14)–C(12)–O(12)–H(12) torsion angle, which is 177° and 70° in H·2TMU and H·2HMPA, respectively. This torsion angle accounts for the difference in channel type and orientation. The same torsion angle in the H·DMF and H·DMA complexes are C(14A)–C(12A)–O(12A)–H(12A) = 81° and 178° and C(14B)–C(12B)–O(12B)–H(12B) = 170° and 85°, respectively. This variation must account for chain formation.

The Hirshfeld surface fingerprint plots [16, 17] for four structures are shown in Fig. 6. In each case the surface only envelops the host molecule. The fingerprint plots of H·DMF (A and B) are closely related to those of H·DMA

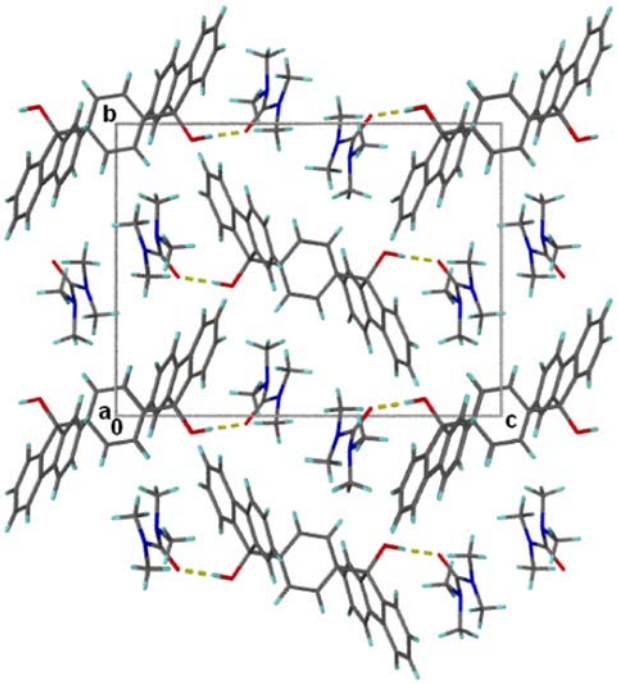

Fig. 4 Packing diagram of H·2TMU down [100] showing the distinct supramolecular host–guest entity. Only one pair of the disordered $-CH_3$ included

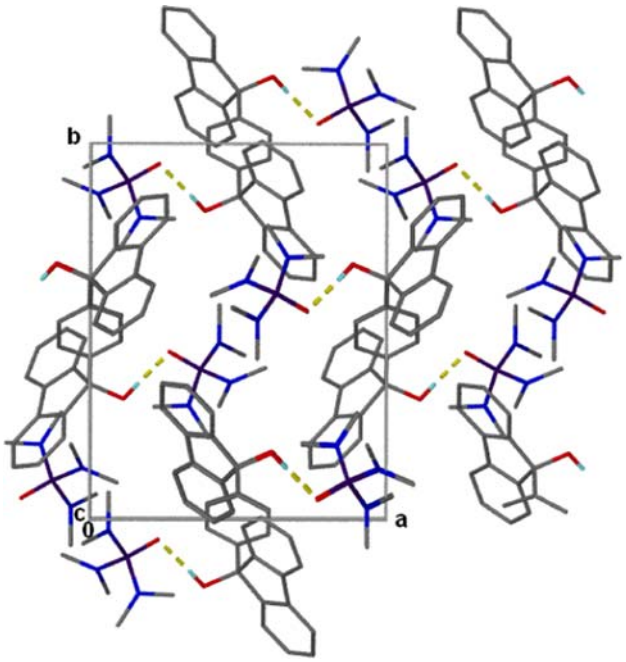

Fig. 5 Packing diagram of H·2HMPA down [001] showing the distinct supramolecular host–guest entity. All hydrogen atoms omitted, for clarity, except the hydroxyl hydrogen atom

and have therefore been excluded. The plots were computed from the Hirshfeld surface using the CrystalExplorer program [18]. From these fingerprint plots one can derive the areas associated with O···H, H···H, C···H and C···C contacts and the frequency of these contacts are summarised in Fig. 7. From this figure it is apparent that the structures have similar interactions, with the number of the O···H interactions increasing upon guest inclusion. One difference, however, is found in H_B which is the only molecule in which C···C contacts or $\pi\cdots\pi$ interaction are observed.

For H_A and H_B, the spike labelled 1, is associated with the O_A–$H_A\cdots O_B$ hydrogen bond. The hydrogen bonding spike features is found in all the plots and is of a similar length in each complex. For the host, the spike labelled 2, with $d_e = d_i \sim 1.08$ Å, is due to intermolecular H···H contacts and this feature, although weaker, is also present in the plot of H·2HMPA. H_B exhibits distinct spikes (labelled 3) associated with C···H contacts which also occur in maps for H·2TMU and H·2HMPA. "Wings" (labelled 4) are seen in all the structures except H·2HMPA and represent C–H···π interactions. The variations observed in the maps can be attributed to the different packing arrangements and structural features found within each complex.

Thermal analysis

The results of TGA and DSC are shown in Fig. 8 and Table 3. The TGA traces shows a single-step desorption, except for the H·2HMPA complex in which desorption is a multi-step process. From the mass loss the H:G ratio was determined and the calculated values corresponded to those observed experimentally.

DSC was used to determine onset temperatures of guest release and to monitor any phase changes occurring in the structures upon heating. The DSC traces of the complexes H·DMF, H·DMA and H·2TMU are similar as endotherm **A** corresponds to desorption which is followed by the melt of the host compound (endotherms **C**). The DSC of the H·2TMU is interesting in that the first endotherm **A** is clearly due to the guest-loss reaction, but endotherm **B** can be assigned to a phase change of the host, followed by the melting endotherm of the host at **C**. This phenomenon has been observed before [19]. The trace of H·2HMPA shows a broad exotherm over the range 115–152 °C. This thermal event represents a recrystallisation of the material.

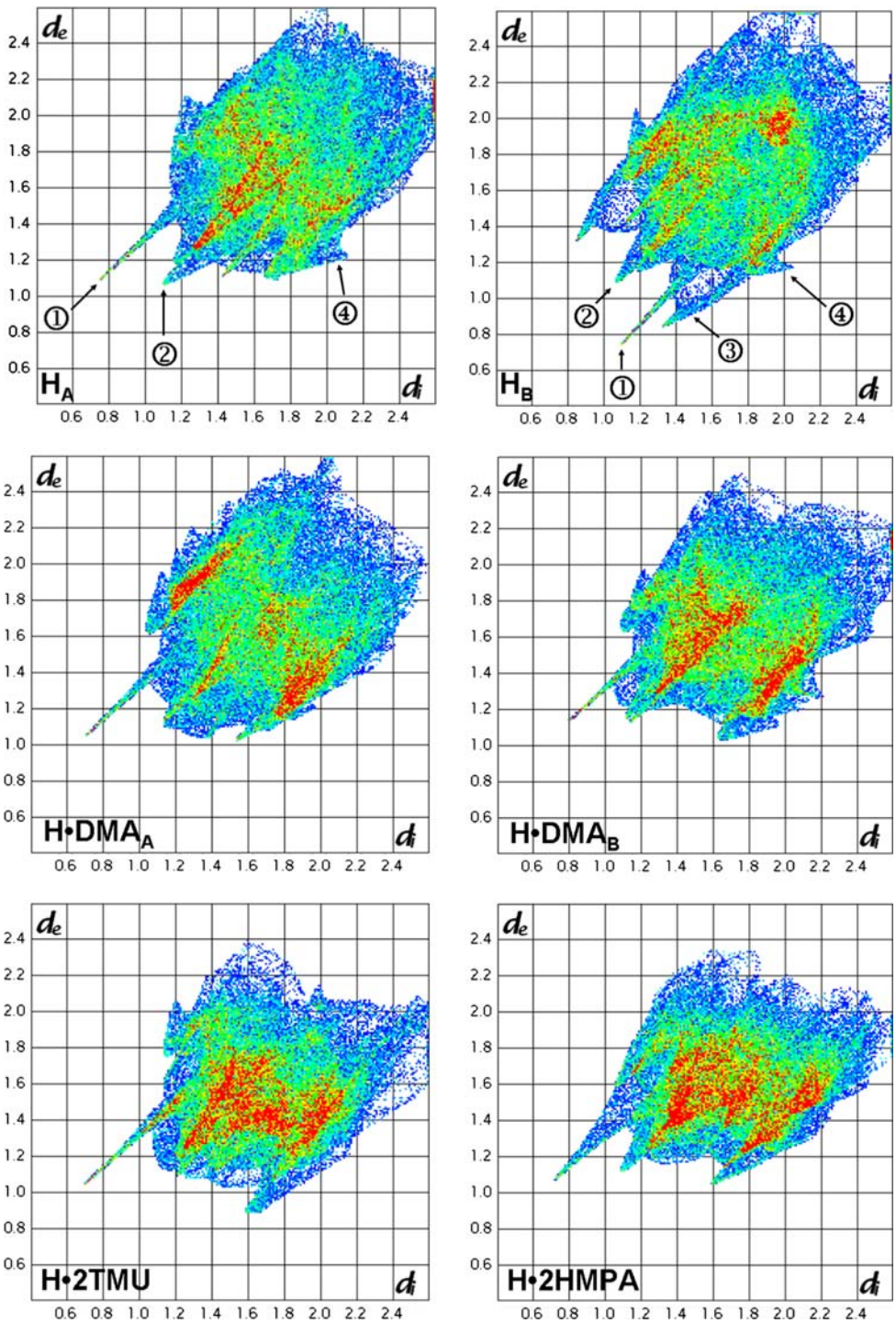

Fig. 6 Hirshfeld fingerprint plots of H (molecules A and B), H·DMA (molecule A and B), H·2TMU and H·2HMPA

Determining the T_{on} of guest release was not accurate as the desorption peaks were broad therefore the first derivative was calculated from the TGA trace as a further means of comparison of the four complexes. These results indicate a measure of the thermal stability of the complexes to be of the order H·DMF > H·DMA > H·2TMU > H·2HMPA.

Lattice energy calculations

Results for the lattice energy calculations are shown in Table 4. These calculation show the stabilities of the inclusion complexes to be in the order H·DMF > H·DMA > H·2TMU > H·2HMPA. This is in agreement with the results obtained from the first derivative curve

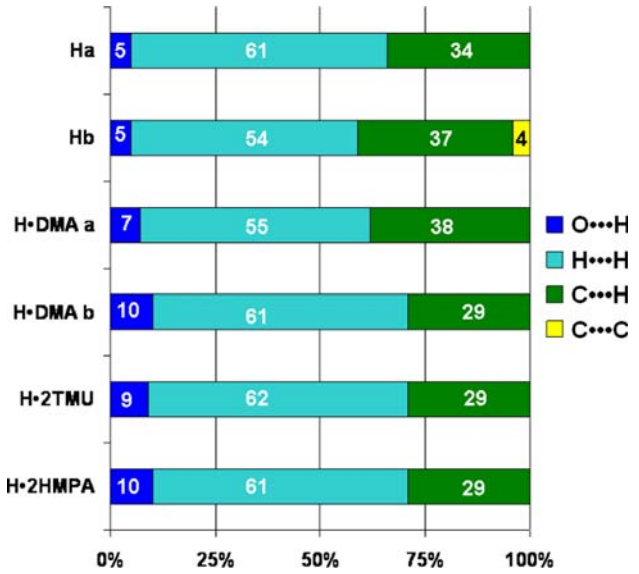

Fig. 7 Relative contribution to the Hirshfeld surface area for the various close intermolecular contacts in H (molecules A and B), H·DMA (molecules A and B), H·2TMU and H·2HMPA

calculated from thermal analysis. We are aware that lattice energy calculations are only strictly valid for host–guest systems which have the same stoichiometry and where the guests are isomeric. We therefore adjusted the results by dividing the lattice energy by the number of electrons in the structure [15]. The values obtained indicated that the trend observed is maintained.

Conclusions

The structure of the inclusion complexes H·DMF and H·DMA are essentially the same, with the guests lying in channels and stabilised by two host–guest hydrogen bonds. Their structural similarities are reflected in their thermal stabilities and lattice energy values. On comparison, the H·2TMU and H·2HMPA structures are thermally less stable and this can be explained by the differences in hydrogen bonding. The double acceptor hydrogen bonding capability of DMF and DMA give these structures more stability. While TMU and HMPA are single acceptor guests and hence only one hydrogen bond needs to be broken on guest release. This series of inclusion complexes shows the important role that hydrogen bonding has on complex stability.

Supporting information

The CIF files for the complexes have been deposited with the Cambridge Crystallographic Data Centre (CCDC 690551–690555 for complexes H, H·DMF, H·DMA,

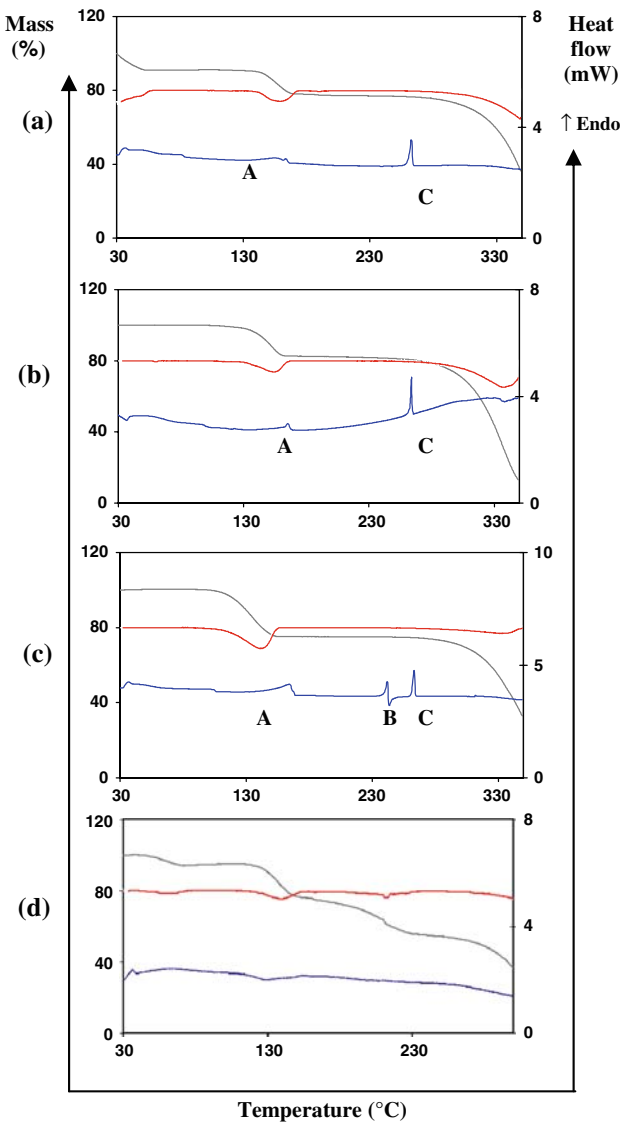

Fig. 8 DSC (bottom), TGA (top) and the first derivative curve of the TGA (middle) of (**a**) H·DMF, (**b**) H·DMA, (**c**) H·2TMU and (**d**) H·2HMPA

Table 3 Thermal analysis results

	H·DMF	H·DMA	H·2TMU	H·2HMPA
TGA results				
Calc. %	14.3	16.6	34.6	44.9
Exp. %	14.4	16.3	30.0	40.8
H:G ratio	1:1	1:1	1:2	1:2
Peak 1st derv. (°C)	160	156	143	140
DSC results				
Peak A T_{on} (°C)	–	158	148	–
Peak B T_{on} (°C)	–	–	242	–
Peak C T_{on} (°C)	263	264	263	–

Table 4 Lattice energy calculation results

	Lattice energy (E) (kJ mol^{-1})	$E \div$ no. of electrons
H	−408.83	−0.89
H·DMF	−577.58	−1.07
H·DMA	−576.62	−1.04
H·2TMU	−366.40	−1.02
H·2HMPA	−362.37	−0.85

H·2TMU and H·2HMPA, respectively). These data may be obtained, on request, from the CCDC, 12 Union Road, Cambridge CB2 1EZ, UK. Tel: +44-1233-336408; fax: +44-1233-336033; e-mail: deposit@ccdc.cam.ac.uk.

Acknowledgments EDV and LRN thank the National Research Foundation of Pretoria and the University of Cape Town for financial assistance.

References

1. Caira, M.R., Jacobs, A., Nassimbeni, L.R., Toda, F.: Complexation with diol host compounds. Part 36: inclusion compounds of 1,1,6,6-tetraphenylhexa-2,4-diyne-1,6-diol with benzene, toluene and mesitylene. J. Chem. Crystallogr. **36**(7), 435–443 (2006). doi:10.1007/s10870-005-9042-8
2. Caira, M.R., Jacobs, A., Nassimbeni, L.R., Toda, F.: Inclusion compounds of 1,1,6,6-tetraphenylhexa-2,4-diyne-1,6-diol with DMF and DMSO: structures, selectivity and kinetics of desolvation. CrystEngComm **5**, 150–153 (2003). doi:10.1039/b302548a
3. Bond, D.R., Johnson, L., Nassimbeni, L.R., Toda, F.J.: Complexation with diol host compounds. Part 6. Structure and dynamics of enclathration by 1,1,6,6-tetraphenyl-hexa-2,4-diyne-1,6-diol. Solid State Chem. **92**(1), 68–79 (1991). doi:10.1016/0022-4596(91)90243-B.
4. Weber, E., Nitsche, S., Wierig, A., Csöregh, I.: Inclusion compounds of diol hosts featuring two 9-Hydroxy-9-fluorenyl or analogous groups attached to linear spacer units. Eur. J. Org. Chem. **2002**(5), 856–872 (2002). doi:10.1002/1099-0690(200203)2002:5<856::AID-EJOC856>3.0.CO;2-R
5. Weber, E.: MacNicol, D.D., Toda, F., Bishop, R. (eds.) Shape and symmetry in the design of new hosts. Comprehensive Supramolecular Chemistry, vol. 6, Chap. 17. Pergamon, Oxford (1996)
6. Weber, E.: In: Atwood, J.L., Davies, J.E.D., MacNicol, D.D. (eds.) Scissor type hosts: molecular design and inclusion behaviour. Inclusion Compounds, vol. 4, Chap. 5. Oxford University Press, Oxford (1991)
7. Bacchi, A., Bosetti, E., Carcelli, M., Pelagatti, P., Rogolino, D., Pelizzi, G.: "Venetian blinds" mechanism of solvation/desolvation in Palladium(II) wheel-and-axle organic-inorganic diols. Inorg. Chem. **44**(2), 431–442 (2005). doi:10.1021/ic048896m
8. Bacchi, A., Bosetti, E., Carcelli, M.: Engineering organic/inorganic diols that reversibly capture and release volatile guests. CrystEngComm **7**, 527–537 (2005). doi:10.1039/b507966g
9. Hooft, R.: COLLECT. Data Collection Software. Nonius BV, Delft, The Netherlands (1998)
10. Otwinowski, Z., Minor, W.: Processing of X-ray diffraction data collected in oscillation mode. Methods Enzymol. **276**, 307–326 (1997). doi:10.1016/S0076-6879(97)76066-X
11. Sheldrick, G.M.: SHELXS86. In: Sheldrick, G.M., Kruger, C., Goddard, P. (eds.) Crystallographic Computing, pp. 3–175. Oxford University Press, Oxford (1985)
12. Sheldrick, G.M.: SHELXL-97. University of Göttingen, Germany (1997)
13. Barbour, L.J.: X-Seed—A software tool for supramolecular crystallography. J. Supramol. Chem. **1**, 189–191 (2001). doi:10.1016/S1472-7862(02)00030-8
14. Atwood, J.L., Barbour, L.J.: Molecular graphics: from science to art. Cryst. Growth Des. **3**, 3–8 (2003). doi:10.1021/cg020063o
15. Gavezzotti, A.: OPIX. University of Milan, Italy (2003)
16. McKinnon, J.J., Spackman, M.A., Mitchell, A.S.: Novel tools for visualizing and exploring intermolecular interactions in molecular crystals. Acta Crystallogr. B **B60**(6), 627–668 (2004). doi:10.1107/S0108768104020300
17. Spackman, M.A., McKinnon, J.J.: Fingerprinting intermolecular interactions in molecular crystals. Cryst. Eng. Comm **4**, 378–392 (2002). doi:10.1039/b203191b
18. Wolff, S.K., Grimwood, D.J., McKinnon, J.J., Jayatilaka, D., Speckman, M.A.: CrystalExplorer 2.0. University of Western Australia, Perth, Australia (2005–2007)
19. Caira, M.R., Nassimbeni, L.R., Vujovic, D., Weber, E., Wierig, A.: Separation of lutidine isomers by inclusion. Struct. Chem. **10**, 205–211 (1999). doi:10.1023/A:1021836513608